COMPUTATIONAL MECHANICS 2023
38th conference with international participation
Srní
October 23 - 25, 2023

Dynamics of a cantilever beam with piezoelectric sensor: Parameter identification

R. Cimrman[a,b], R. Kolman[a,c], L. Musil[a], V. Kotek[a], J. Kylar[a]

[a] *Institute of Thermomechanics, Czech Academy of Sciences, Dolejškova 1402/5, 18200, Praha 8, Czech Republic*
[b] *New Technologies Research Centre, University of West Bohemia, Univerzitní 8, 301 14 Plzeň, Czech Republic*
[c] *College of Polytechnics Jihlava, Tolstého 16, 586 01 Jihlava, Czech Republic*

The piezoelectric materials are electroactive materials often applied for real-time sensing or structural health monitoring. Mathematical models of such structures contain several material parameters that need to be identified from experiments. The (proportional) damping coefficients are an example of such parameters, difficult to obtain in another way.

Our aim was to develop a computer model of a simple experiment performed in our laboratory [6] involving dynamics of a cantilever beam with an attached piezoelectric sensor excited by a suddenly removed weight, see Figs. 1–2. The sensor was connected to an oscilloscope that measured the voltage on the top side of the sensor, the bottom side was grounded. We had been interested in correctly simulating the experiment for various materials of the beam and/or in identifying parameters that were unknown or uncertain in advance. Preliminary simulations revealed that the oscilloscope had a finite resistance, motivating us to augment the model presented in [4]. The new model is briefly summarized below.

Let us denote by Ω_E the elastic part and by Ω_P the piezoelectric part of a body with $\Omega \subset \mathbb{R}^3$, see Fig. 1. The weak formulation of the model is as follows. Let $V_0^u(\Omega) = \{\boldsymbol{u} \in [H^1(\Omega)]^3, \boldsymbol{u} = \boldsymbol{0} \text{ on } \Gamma_u\}$, $V_0^\varphi = \{\varphi \in H^1(\Omega), \varphi = 0 \text{ on } \Gamma_{p0}\}$. We seek $\boldsymbol{u}(t)$, $\varphi(t)$, $\bar{\varphi}(t)$ such that

$$\int_\Omega \rho \boldsymbol{v} \cdot \ddot{\boldsymbol{u}} + \int_\Omega \boldsymbol{\varepsilon}(\boldsymbol{v})^T \boldsymbol{C} \boldsymbol{\varepsilon}(\boldsymbol{u}) + \alpha \int_\Omega \rho \boldsymbol{v} \cdot \dot{\boldsymbol{u}} + \beta \int_\Omega \boldsymbol{\varepsilon}(\boldsymbol{v})^T \boldsymbol{C} \boldsymbol{\varepsilon}(\dot{\boldsymbol{u}}) - \int_{\Omega_P} \boldsymbol{\varepsilon}(\boldsymbol{v})^T \boldsymbol{e}^T \boldsymbol{\nabla} \varphi - \int_\Omega \boldsymbol{v} \cdot \boldsymbol{b} = 0 \qquad \forall \boldsymbol{v} \in V_0^u(\Omega) , \tag{1}$$

$$\int_{\Omega_P} (\boldsymbol{\nabla} \psi)^T \boldsymbol{e} \boldsymbol{\varepsilon}(\boldsymbol{u}) + \int_{\Omega_P} (\boldsymbol{\nabla} \psi)^T \boldsymbol{\kappa} \boldsymbol{\nabla} \varphi - \int_{\Gamma_{pQ}} (\boldsymbol{\kappa} \boldsymbol{\nabla} \varphi) \cdot \boldsymbol{n} \psi + \int_{\Gamma_{pQ}} (\boldsymbol{\kappa} \boldsymbol{\nabla} \psi) \cdot \boldsymbol{n} (\varphi - \bar{\varphi}) = 0 \qquad \forall \psi \in V_0^\varphi(\Omega) , \tag{2}$$

$$\int_{\Gamma_{pQ}} (\boldsymbol{\kappa} \boldsymbol{\nabla} \dot{\varphi}) \cdot \boldsymbol{n} + \bar{\varphi}/R = 0 , \tag{3}$$

$$\boldsymbol{u} = 0 \qquad \text{on } \Gamma_u \times [0, T] , \tag{4}$$

$$\varphi = 0 \qquad \text{on } \Gamma_{p0} \times [0, T] , \tag{5}$$

$$\boldsymbol{u}(0) = \boldsymbol{u}^0,\ \dot{\boldsymbol{u}}(0) = 0,\ \varphi(0) = \varphi^0 \qquad \text{in } \Omega , \tag{6}$$

where $\boldsymbol{u}$ is the mechanical displacement vector inducing the Cauchy strain $\boldsymbol{\varepsilon}$, φ is the electric potential, $\bar{\varphi}$ is the unknown potential on the top side of the sensor Γ_{pQ}, ρ is the density. $\boldsymbol{C}$ is the matrix of elastic properties (under constant electric field intensity in Ω_P), α, β are the

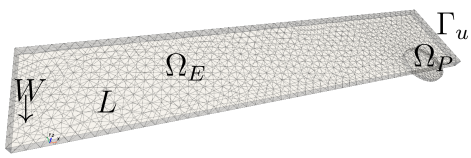

Fig. 1. The computational mesh. A weight is attached to the bottom side at the point W at time $t = 0$ s. Dynamic quantities are recorded in the point L

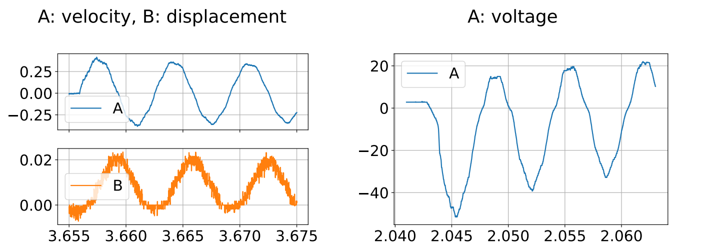

Fig. 2. The experimental data: (left) laser vibrometer, (right) oscilloscope

proportional damping coefficients, $\boldsymbol{e}$ the piezoelectric modulus, $\boldsymbol{\kappa}$ the permittivity under constant deformation and $\boldsymbol{n}$ is the unit outward normal. The structure is loaded by the self-weight volume forces $\boldsymbol{b}$. The initial conditions $\boldsymbol{u}^0$, φ^0 correspond to a static loading of the body by a localized surface force of a weight (280 g) attached, using a nylon string, at point W in Fig. 1. The external circuit is modeled by (3) with R being the oscilloscope resistance. The last two terms in (2) correspond to the weak enforcement of the Dirichlet boundary condition $\varphi = \bar{\varphi}(t)$ on Γ_{pQ} using the non-symmetric Nitsches method [8] without the penalty term [2].
The finite element discretization of (1)–(3) uses

$$\boldsymbol{u}(\boldsymbol{\xi}) = \mathbf{N}_u(\boldsymbol{\xi})\mathbf{u} \;, \quad \varphi(\boldsymbol{\xi}) = \mathbf{N}_\varphi(\boldsymbol{\xi})\mathbf{p} \;, \quad \bar{\varphi} = 1\bar{p} \;, \tag{7}$$

where $\mathbf{N}_u(\boldsymbol{\xi})$, $\mathbf{N}_\varphi(\boldsymbol{\xi})$ are the displacement and the potential shape functions, respectively. The implicit second order Newmark method [7] is used to discretize the dynamical part (1), while the central difference scheme is used for (3). Because we want to perform a sensitivity analysis of the time-dependent system on several problem parameters, we present the discrete equations in the extended form with the unknowns vectors $\mathbf{u}$, $\dot{\mathbf{u}}$, $\ddot{\mathbf{u}}$, $\mathbf{p}$, $\dot{\mathbf{p}}$, $\bar{p}$ of the time step n, the $n-1$ time step quantities indicated by the superscript ^{0}

$$\ddot{\mathcal{U}}: \quad \mathbf{M}\ddot{\mathbf{u}} + \mathbf{C}\dot{\mathbf{u}} + \mathbf{K}\mathbf{u} - \mathbf{B}^T\mathbf{p} - \mathbf{b} = 0 \;, \tag{8}$$

$$\mathcal{P}: \quad \mathbf{B}\mathbf{u} + (\mathbf{D} - \mathbf{F} + \mathbf{F}^T)\mathbf{p} - \mathbf{F}^T\mathbf{1}\bar{p} = 0 \;, \tag{9}$$

$$\bar{\mathcal{P}}: \quad \mathbf{1}^T\mathbf{F}\dot{\mathbf{p}} + \frac{1}{2R}(\bar{p} + \bar{p}^0) = 0 \;, \tag{10}$$

$$\dot{\mathcal{U}}: \quad \dot{\mathbf{u}} - \dot{\mathbf{u}}^0 - (1-\gamma_N)\Delta t\ddot{\mathbf{u}}^0 - \gamma_N\Delta t\ddot{\mathbf{u}} = 0 \;, \tag{11}$$

$$\mathcal{U}: \quad \mathbf{u} - \mathbf{u}^0 - \Delta t\dot{\mathbf{u}}^0 - (\frac{1}{2} - \beta_N)\Delta t^2\ddot{\mathbf{u}}^0 - \beta_N\Delta t^2\ddot{\mathbf{u}} = 0 \;, \tag{12}$$

$$\dot{\mathcal{P}}: \quad \dot{\mathbf{p}} + \frac{1}{\Delta t}\mathbf{p}^0 - \frac{1}{\Delta t}\mathbf{p} = 0 \;, \tag{13}$$

where $\mathbf{M}$ is the mass matrix, $\mathbf{C}$ is the damping matrix, $\mathbf{K}$ is the stiffness matrix, $\mathbf{B}$ is the piezoelastic coupling matrix, $\mathbf{D}$ is the electrostatic potential matrix and $\mathbf{b}$ is the volume forces vector. The surface flux matrix $\mathbf{F} = \int_{\Gamma_{pQ}} \mathbf{N}_\varphi^T \boldsymbol{n}\boldsymbol{\kappa}\mathbf{N}_\varphi'$ is used to impose weakly the Dirichlet boundary condition $\varphi = \bar{\varphi}$ on Γ_{pQ}, $\mathbf{1}$, the matrix of ones, is used to sum the rows of $\mathbf{F}$, performing thus the integration of (3). The Newmark scheme is expressed by (11), (12), β_N, γ_N are its parameters, the central difference scheme by (13) and the average in the second term of (10). When computing the direct problem, $\dot{\mathbf{u}}$, $\mathbf{u}$, $\dot{\mathbf{p}}$ expressed from (11)–(13) are substituted into (8)–(10), resulting in three primary unknowns $\ddot{\mathbf{u}}$, $\mathbf{p}$, $\bar{p}$ to compute in each time step by solving a linear system.

The parameter identification is done by fitting a time series of measured data – in our case the velocity component $v_z(t)$ measured by a laser vibrometer in the point L – to the corresponding simulated quantity $\dot{u}_z(L,t)$ by a nonlinear least-squares solver (`least_squares()` function from SciPy [10]). This solver can compute the Jacobian matrix of the objective function F numerically or use a user-supplied function returning partial sensitivities. For our linear problem, we do not expect to achieve a faster elapsed time with a semi-analytical Jacobian matrix (see below) than with the default 2-point finite difference scheme, because the number of linear systems to solve is the same and computing the Jacobian analytically involves some additional calculations. Nevertheless it allows us to test our automatically differentiated terms based on JAX [1] and provides a proof-of-concept for future nonlinear extensions of the model.

The state problem (8)–(13) in an abstract form (see also [9]) can be written as

$$\Phi(\boldsymbol{\alpha}, \mathbf{y}, \mathbf{y}^0) = 0 \;, \quad \mathbf{y} \equiv [\mathbf{u}, \dot{\mathbf{u}}, \ddot{\mathbf{u}}, \mathbf{p}, \dot{\mathbf{p}}, \bar{p}]^T \;, \tag{14}$$

where $\boldsymbol{\alpha}$ are the parameters to be identified. Our aim is to calculate the partial sensitivities $\frac{\partial \dot{u}_z(L,t)}{\partial \alpha}$. By differentiating (14) w.r.t. $\boldsymbol{\alpha}$ a recurrent relation

$$\frac{\partial \Phi}{\partial \mathbf{y}} \frac{\partial \mathbf{y}}{\partial \boldsymbol{\alpha}} = -\left(\frac{\partial \Phi}{\partial \boldsymbol{\alpha}} + \frac{\partial \Phi}{\partial \mathbf{y}^0} \frac{\partial \mathbf{y}^0}{\partial \boldsymbol{\alpha}}\right) \tag{15}$$

is obtained allowing us to compute $\frac{\partial \mathbf{y}}{\partial \boldsymbol{\alpha}}$ in all time steps, initialized by using the initial conditions. Then $\frac{\partial \dot{u}_z(L,t)}{\partial \alpha}$ are simply a component in $\frac{\partial \mathbf{y}}{\partial \boldsymbol{\alpha}}$.

To briefly demonstrate the parameter identification, below we identify the parameters β (the stiffness proportional damping parameter), E (the Young's modulus of the beam) and u_0 (a scalar multiplier of the initial condition $\boldsymbol{u}^0$), using preliminary data for $t = [0, 0.02]$ s with the following (initial) material parameters:

- Steel elastic beam: $\rho = 7800$ kg/m^3, $E = 210$ GPa, $\nu = 0.3$.
- Piezoelectric disc: $\rho = 7800$ kg/m^3, the vacuum permittivity $\varepsilon^0 = 8.8541878128 \cdot 10^{-12}$ F/m and

$$\text{in Voigt notation: } \boldsymbol{C}^P = \begin{bmatrix} 127.2050 & 80.2122 & 84.6702 & 0.0000 & 0.0000 & 0.0000 \\ 80.2122 & 127.2050 & 84.6702 & 0.0000 & 0.0000 & 0.0000 \\ 84.6702 & 84.6702 & 117.4360 & 0.0000 & 0.0000 & 0.0000 \\ 0.0000 & 0.0000 & 0.0000 & 22.9885 & 0.0000 & 0.0000 \\ 0.0000 & 0.0000 & 0.0000 & 0.0000 & 22.9885 & 0.0000 \\ 0.0000 & 0.0000 & 0.0000 & 0.0000 & 0.0000 & 23.4742 \end{bmatrix} \text{GPa},$$

$$\boldsymbol{e} = \begin{bmatrix} 0.00000 & 0.00000 & 0.0000 & 0.0000 & 17.0345 & 0.0 \\ 0.00000 & 0.00000 & 0.0000 & 17.0345 & 0.0000 & 0.0 \\ -6.62281 & -6.62281 & 23.2403 & 0.0000 & 0.0000 & 0.0 \end{bmatrix} \text{C/m}^2, \boldsymbol{\kappa} = \varepsilon^0 \begin{bmatrix} 1704.4 & 0.0 & 0.0 \\ 0.0 & 1704.4 & 0.0 \\ 0.0 & 0.0 & 1433.6 \end{bmatrix} \text{F/m}\,.$$

All results were obtained using the Open Source finite element software SfePy [5, 3]. The convergence of the identification procedure is shown in Fig. 3 (left), where the evolution of the parameters and the l^2 norm of the objective function are depicted. The initial and identified time histories of $\dot{u}_z(L,t)$ are shown in Fig. 3 (right), together with the experimental data. The initial parameters correspond to reference values (a steel beam) and the attached weight loading. The results indicate some discrepancies in the experiment: the initial deflection of the beam should have been higher, see u_0, to explain the amplitude of the data, and the elastic beam Young's modulus E lower to match the principal frequency of the data. Note that the decreased Young's modulus E does not explain the initial amplitude by itself. Based on that, new experiments are being undertaken, where e.g. the influence on the applied initial load of cutting the nylon string of the weight is decreased, and the material parameters of the beam are determined experimentally instead of using reference material data from a data sheet. Finally, the proportional damping coefficient was determined to be about 1.92×10^{-5} s.

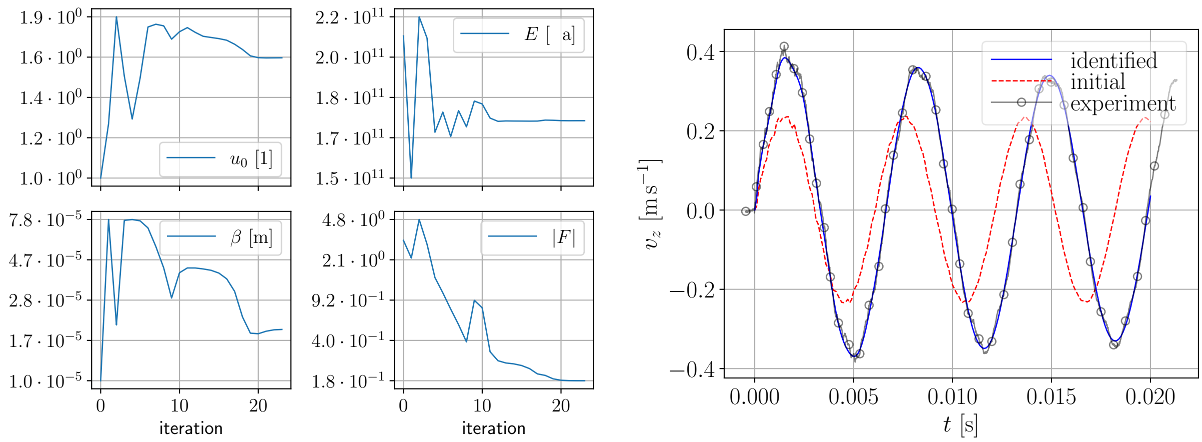

Fig. 3. Parameter identification: (left) the evolution of parameters and objective function during the objective function calls; (right) experiment, original and identified $\dot{u}_z(L, t)$

Acknowledgement

This work has been supported by the grant 23-06220S of the Czech Science Foundation within institutional support RVO:61388998.

References

[1] Bradbury, J., Frostig, R., et al., JAX: Composable transformations of Python+NumPy programs, https://github.com/google/jax, 2023. Ver. 0.4.14.

[2] Burman, E., A penalty-free nonsymmetric nitsche-type method for the weak imposition of boundary conditions, SIAM Journal on Numerical Analysis 50 (4) (2012) 1959-1981.

[3] Cimrman, R., Fast evaluation of finite element weak forms using python tensor contraction packages, Advances in Engineering Software 159 (2021) No. 103033.

[4] Cimrman, R., Kolman, R., Musil, L., Kotek, V., Kylar, J., Dynamics of a cantilever beam with piezoelectric sensor: Finite element modeling, Proceedings of the 29th International Conference Engineering Mechanics 2023, Milovy, May 9-11, 2023, (editors) V. Radolf, I. Zolotarev, Institute of Thermomechanics of the Czech Academy of Sciences, 2023, pp. 51-54.

[5] Cimrman, R., Lukeš, V., Rohan, E., Multiscale finite element calculations in Python using SfePy, Advances in Computational Mathematics 45 (2019) 1897-1921.

[6] Kolman, R., Kylar, J., Kotek, V., Cimrman, R., Musil, L., Dynamics of a cantilever beam with piezoelectric sensor: Experimental study, Proceedings of the 29th International Conference Engineering Mechanics 2023, Milovy, May 9-11, 2023, (editors) V. Radolf, I. Zolotarev, Institute of Thermomechanics of the Czech Academy of Sciences, 2023, pp. 119–122.

[7] Newmark, N. M., A method of computation for structural dynamics, Journal of the Engineering Mechanics Division 85 (3) (1959) 67-94.

[8] Nitsche, J., About a variation principle for solving the Dirichlet problem when using subspaces that are not subject to boundary conditions, Abhandlungen aus dem Mathematischen Seminar der Universität Hamburg 36 (1) (1971) 9-15. (in German)

[9] Rohan, E., Cimrman, R., Sensitivity analysis and material identification for activated smooth muscle, Computer Assisted Mechanics and Engineering Sciences Vol. 9, No. 4 (2002) 519–541.

[10] Virtanen, P., Gommers, R., Oliphant, T. E., Haberland, M., Reddy, T., Cournapeau, D., Burovski, E., Peterson, P., Weckesser, W., Bright, J., van der Walt, S. J., Brett, M., Wilson, J., Millman, K. J., Mayorov, N., Nelson, A. R. J., Jones, E., Kern, R., Larson, E., Carey, C. J., Polat, I., Feng, Y., Moore, E. W., VanderPlas, J., Laxalde, D., Perktold, J., Cimrman, R., Henriksen, I., Quintero, E. A., Harris, C. R., Archibald, A. M., Ribeiro, A. H., Pedregosa, F., van Mulbregt, P., SciPy 1.0: fundamental algorithms for scientific computing in Python, Nature Methods 17 (33) (2020) 261-272.